Ban. J. Med. Phys., Vol -16, Issue -1, 2025 : 1-6

ORIGINAL ARTICLE

BANGLADESH JOURNAL OF MEDICAL PHYSICS

Journal Homepage: www.banglajolinfo/index.php/bjmp

Application of PHITS Code to Design Linear Accelerator and its Bunker

Md. Mojahidul Islam[1], H. M. Waliullah[1], Md. Masud Rana[1], Hiroshi Watabe[2] and M Rafiqul Islam[3] *

[1]*Department of Physics, Mohammadpur Kendriya College, National University, Bangladesh*

[2]*Research Center for Accelerator and Radioisotope Science, Sendai, Japan*

[3]*Institute of Nuclear Medical Physics, Atomic Energy Research Establishment, Bangladesh Atomic Energy Commission, Dhaka, Bangladesh*

ARTICLE INFO

Article history:
Received : **12 May 2025**
Received in revised form : **14 June 2025**
Accepted : **21 June 2025**
Available online : **01 July 2025**

Key words:
Radiotherapy, Linear Accelerator, PHITS, Shielding Design, Particle Tracking
doi: https://doi.org/10.3329/bjmp.v16i1.84795
Article Category: **Radiation Protection**

Corresponding author:
M Rafiqul Islam
mripbaec@gmail.com

ABSTRACT

This study utilized the Particle and Heavy Ion Transport code System (PHITS) Monte Carlo code to develop a computer model of a Varian CLINAC (iX) linear accelerator (LINAC) operating at 6 MV and to design the shielding for its treatment bunker. The LINAC head, comprising the target, primary collimator, flattening filter, and secondary collimator, was accurately modeled based on manufacturer specifications. A water phantom was incorporated to calculate the Percentage Depth Dose (PDD) and beam profiles for a 10×10 cm² field at a Source-to-Surface Distance (SSD) of 100 cm. The success of the model was validated by visualizing particle tracks (photons, electrons, neutrons). The maximum dose was found at a depth of 1.5 cm in water for a 6 MV beam. Furthermore, a comprehensive 3D model of a radiotherapy bunker was constructed using PHITS, with shielding composed of concrete and lead. Simulations confirmed that the designed shielding effectively reduced photon and electron doses to acceptable safety limits outside the bunker. No neutron production was observed at 6 MV, as expected. This work shows how PHITS can be applied to LINAC modeling and shielding assessment under the stated assumptions.

1. Introduction

For over a century, radiation therapy has remained a central pillar in the treatment of cancer [1]. External beam radiotherapy, delivered primarily by medical linear accelerators (LINACs), is a prevalent and effective method for eradicating malignant cells [2]. A LINAC generates high-energy X-ray or electron beams that are precisely targeted at tumors while sparing surrounding healthy tissues to the greatest extent possible [3].

The accuracy of radiotherapy treatment planning is paramount, relying heavily on detailed knowledge of the beam's characteristics, such as the Percentage Depth Dose (PDD) and off-axis dose profiles [4]. While these parameters are measured during machine commissioning, Monte Carlo (MC) simulations have emerged as an indispensable tool for modeling radiation transport, providing a deep understanding of beam physics and offering a virtual platform for testing and validation [5,6]. Furthermore, the high-energy radiation produced by LINACs necessitates robust shielding designs for the treatment bunkers to protect occupational workers and the public from unnecessary exposure [7]. Shielding calculations must account for primary, scattered, and leakage radiation [8]. Traditional methods rely on analytical formulae, but Monte Carlo techniques offer a more rigorous and realistic approach by simulating the actual transport of particles through complex geometries [9].

The aim of this study was employed the PHITS Monte Carlo code to model a Varian CLINAC (iX) LINAC head and simulate its bunker to evaluate photon and electron shielding, ensuring compliance with regulatory dose limits.

2. Materials and Methods

The study was conducted using a Varian CLINAC (iX) LINAC installed at the Institute of Nuclear Medical Physics (INMP), Bangladesh Atomic Energy Commission,

Savar, Dhaka. This machine offers two photon energies (6 MV and 15 MV) and five electron energies (4, 6, 9, 12, 18 MeV). For this work, all measurements and simulations were performed for the 6 MV photon beam. The PHITS code was installed on a computer with Intel core i7 2450 M CPU and 1.8 GHz processor, the operating system windows 10 version 10.0.19045 and the system type 64 bit. The installed physical memory (RAM) is 16.0 GB.

2.1. PHITS Monte Carlo Simulation

The Particle Heavy Ion Transport System (PHITS) is a Monte Carlo method developed by the Japan Atomic Energy Agency (JAEA) to simulate nuclear processes in various research fields such as dosimetry, accelerator, shield design, space research, medical applications, and material research [10]. The geometry (cell and surface), material, and tally are created in one input file to obtain the spectrum in the desired region. The simulation output was produced from two tallies, t-track and t-cross, to visualize the trajectory of particles and to score the particles crossing a cell, respectively. This code provides robust visualization capabilities to ensure the accuracy of the simulation geometry [11]. For this simulation, PHITS version 3.2, the latest available version, was applied.

2.2. LINAC Head Modeling The LINAC head was modeled based on the Varian CLINAC (iX) specifications shown in **Fig. 1(a)**. The key components included in the simulation were:

- **Target:** Made of pure Tungsten (W).
- **Primary Collimator:** Composed of a tungsten-nickel-iron alloy.
- **Flattening Filter:** Made of Copper (Cu).
- **Secondary Collimator (Jaws):** Same material as the primary collimator.

The material compositions and densities are detailed in **Table 1**.

Table 1: Material composition of LINAC head components. [12]

Component	Materials	Percentage (%)	Density (g/cm³)
Target	Tungsten (W-184)	100	19.4
Primary Collimator	Tungsten (W-184)	90.5	17.0
	Nickel (Ni-58)	6.5	
	Iron (Fe-56)	3.0	
Flattening Filter	Copper (Cu-63,65)	69.17	8.92
	Tungsten (W-184)	30.83	
Secondary Collimator	Identical to Primary Collimator		17.0

The geometry was defined using PHITS surface and cell cards. A mono-energetic 6 MeV electron source with a Gaussian spatial distribution (σ = 1 mm) was directed onto the target to generate bremsstrahlung photons.

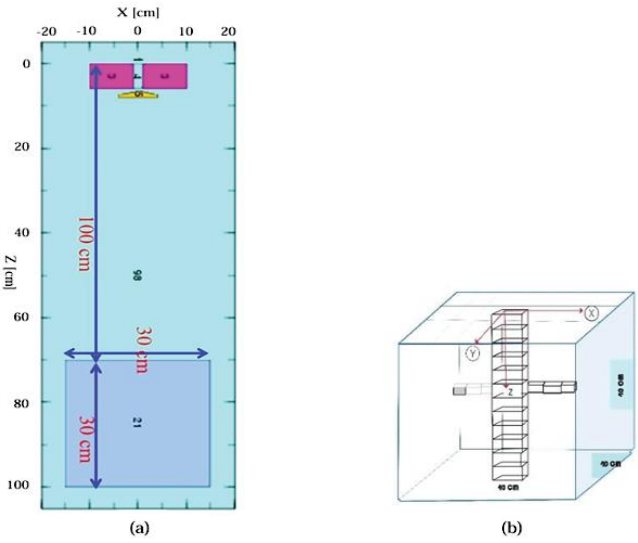

Figure 1: (a) Modeling LINAC head and water phantom with using PHITS and (b) Voxelated water phantom was applied for PDD and lateral beam profile measurements.

On the other hand, to ensure treatment accuracy, phantoms are essential for absolute dosimetry verification and routine quality assurance checks. [13]. A water phantom measuring 30×30×30 cm³ was modeled downstream of the LINAC head. The phantom was voxelized into 1 cm³ cubes to score dose deposition shown in **Fig. 1(a)** and **1(b)**. PDD was calculated along the central axis (z-depth) from the surface to 30 cm depth. Beam profiles were calculated perpendicular to the central axis (x-axis) at a depth of 10 cm. The field size was set to 10×10 cm² at an SSD of 100 cm.

The PDD was calculated using the standard formula Eq-1[14]:

$$\text{PDD (d)} = 100\times \frac{D_d}{D_{dmax}} \quad (1)$$

Where, D_d is absorption dose at the depth d and D_{dmax} is the maximum absorption dose.

In this case, the flatness value is calculated according to Eq-2[15]:

$$F = \frac{D_{max} - D_{min}}{D_{max} + D_{min}} \times 100\% \quad (2)$$

D_{max} = maximum dose in the defined central region, D_{min} = minimum dose in that same region

2.3. Bunker Shielding Modeling

A standard radiotherapy bunker layout was modeled in PHITS based on NCRP guidelines [7, 8]. The bunker geometry included:

- **Primary Barriers:** The primary barrier is the wall into which the beam is incident directly and all other barriers are considered secondary [16]. The primary beam, made of concrete (density 2.35 g/cm³).
- **Secondary Barriers:** Walls shielded from the primary beam but exposed to leakage and scatter, also made of concrete.
- **Maze:** A labyrinthine entrance to attenuate scattered radiation before reaching the door.
- **Door:** Modeled as lead (Pb, density 11.35 g/cm³).

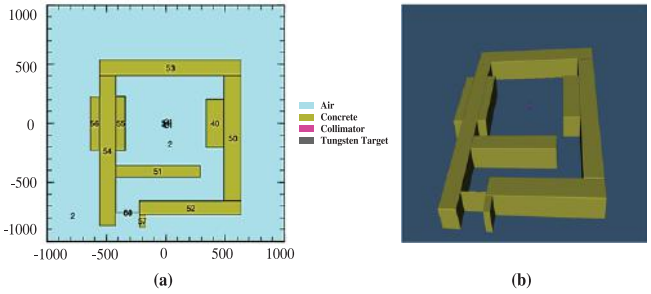

Fig. 2: (a) 2D view of LINAC shielding bunker using PHITS and (b) 3D visualization of shielding bunker with PHITS code.

Fig. 2(a) and **(b)** show the 2D and 3D visualization of the simulated shielding bunker. The entire interior space was defined as air. The LINAC isocenter was placed at the center of the treatment room. Dose scoring tallies were placed at various locations outside the bunker to assess the effectiveness of the shielding.

3. Results and Discussion

3.1 LINAC Head Modeling

The 3D model of the LINAC head generated in PHITS is shown in **Fig. 3**. The visualization successfully depicts the key components and the trajectories of particles as they originate from the target and interact with each component. The modeling of the LINAC therapy device is focused on the LINAC head. This section is chosen because it is the place where X-ray is generated [17].

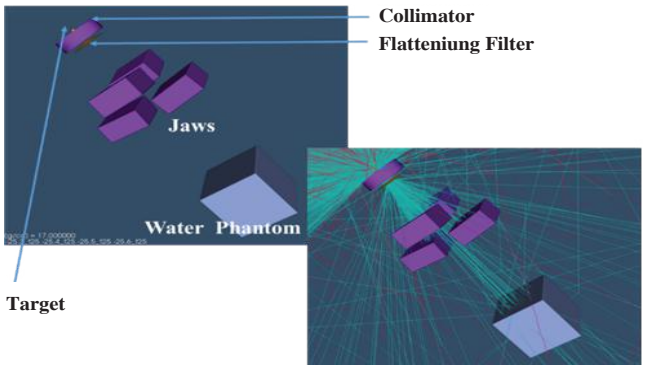

Figure 3: 3D visualization of the LINAC head model with particle tracks.

3.2 Simulated Particle Tracking

Fig. 4(a) shows the 2D visualization of photon tracks in the YZ plane. High-energy electrons striking a tungsten target generate intense X-ray radiation due to tungsten's high atomic number, as higher-Z targets yield more X-rays than lower-Z materials. The high-intensity photon flux (red) is generated at the target via bremsstrahlung interactions. The continuous curve produced by the interaction of electrons with the target is called the Bremsstrahlung curve [18]. The photons are then shaped and filtered by the primary collimator and flattening filter, resulting in a uniform, flattened beam profile as they exit the head toward the phantom. The highest photon flux intensity generated about the target is 10^{-3} 1/cm^2.s (shown in red) and decreases further from the source and down to 10^{-10} 1/cm^2.s (light blue) as it reaches the water phantom.

Fig. 4(b) shows the tracks of secondary electrons generated from photon interactions within the LINAC head components. Photon beams from radiotherapy units (Co-60 or LINAC), in fact, are no longer pure photon beams, but a mixture of photons and a small amount of electrons produced by the photon beams [19]. Doses in build-up region increase due to secondary charged particles (electrons and positrons) that are released in the phantom by photon interactions (i.e. photoelectric effect, Compton effect, and pair production) [20].These contaminant electrons are mostly absorbed by the components and air, with a small fraction reaching the phantom surface.

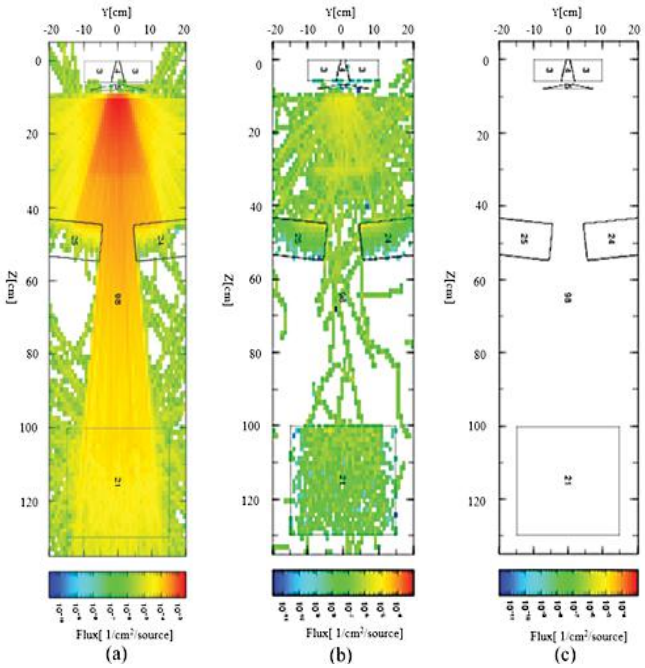

Fig. 4: Figure 4: 2D visualization of (a) Photon tracking, (b) Electron tracking and (c) Neutron Tracking YZ plane. The color scale represents flux intensity.

Fig. 4(c) shows the simulation results show that the interaction of X-ray photons with the LINAC head components at 6 MV does not produce neutrons. There are no photoneutrons at 6 MV‟ result as a sanity check of the physics setup (as expected from (γ,n) thresholds), not as validation of the overall model. This is because at a voltage of 6 MV the X-ray photon energy is smaller than the threshold energy of the target (Threshold energy Cu= 9.91 MeV) [21].

As a result, no neutrons are released from the atomic nuclei during interactions. This validates the model's physics and aligns with clinical practice where neutron shielding is not a concern for 6 MV LINACs.

3.3 Simulated Percentage Depth Dose (PDD) and Beam Profile

The simulated PDD curve for the 6 MV photon beam is presented in **Fig. 5(a)**. In radiotherapy studies, PDD is essential for evaluating how X-ray photon dose is distributed along the LINAC's main axis (z-axis). PDD was calculated from the surface of the water phantom down to a depth of 30 cm. The curve exhibits the characteristic features of a megavoltage beam: a low surface dose, a dose build-up region, a maximum dose (D_{max}) at a depth of 1.5 cm, and an exponential decrease beyond D_{max}. This result shows excellent agreement with the experimental PDD data measured on the physical machine.

characteristic of a well-collimated beam. The symmetry was calculated to be 1.9%, which is within clinical acceptability standards (<3%). This further validates the accuracy of the modeled collimators and flattening filter. The dose profile tends to decrease as it approaches the edge of the irradiation field. This decrease is due to the penumbra effect [20].

3.4: Particle Transport and Dose Mapping for Shielding Effectiveness

Fig. 6(a), **6(b)** and **6(c)** show the 2D visualization of photon, electron and neutron tracking within the bunker's XZ plane, respectively.

- **Photons:** The primary photon beam is fully attenuated by the primary concrete barrier. Scattered and leakage photons are shown hitting the secondary barriers and maze walls. The maze design effectively attenuates these photons through multiple scatterings, preventing them from reaching the entrance door.
- **Electrons:** Secondary electrons generated in the air and from interactions with the head are also tracked. These electrons have very short ranges and are completely stopped by the concrete walls and air, posing no shielding challenge.
- **Neutron:** The simulation confirms that at 6 MV, X-ray photons lack sufficient energy to exceed the neutron production threshold (e.g., Cu = 9.91 MeV), so no neutrons are generated in the LINAC head. This validates the model and matches clinical practice, where neutron shielding is unnecessary for 6 MV beams.

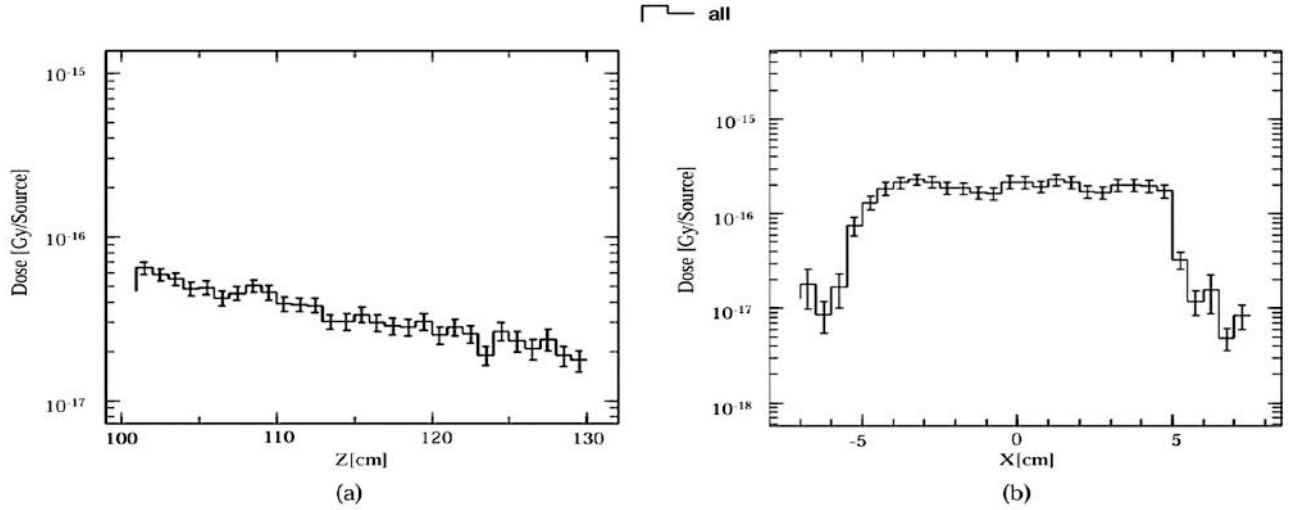

Fig. 5: Simulated (a) Percentage Depth Dose (PDD) curve and (b) beam profile for a 6 MV, 10x10 cm² field at SSD=100 cm. At a time, the simulated beam profile at a depth of 10 cm is shown in **Fig. 5(b)**.

At a time, the simulated beam profile at a depth of 10 cm is shown in Fig. 5(b). The beam profile shows how accurately the LINAC is modeled in the simulation. The flattening filter and collimators have the most influence on the beam shape. The profile is flat and symmetric, with a steep dose fall-off at the edges,

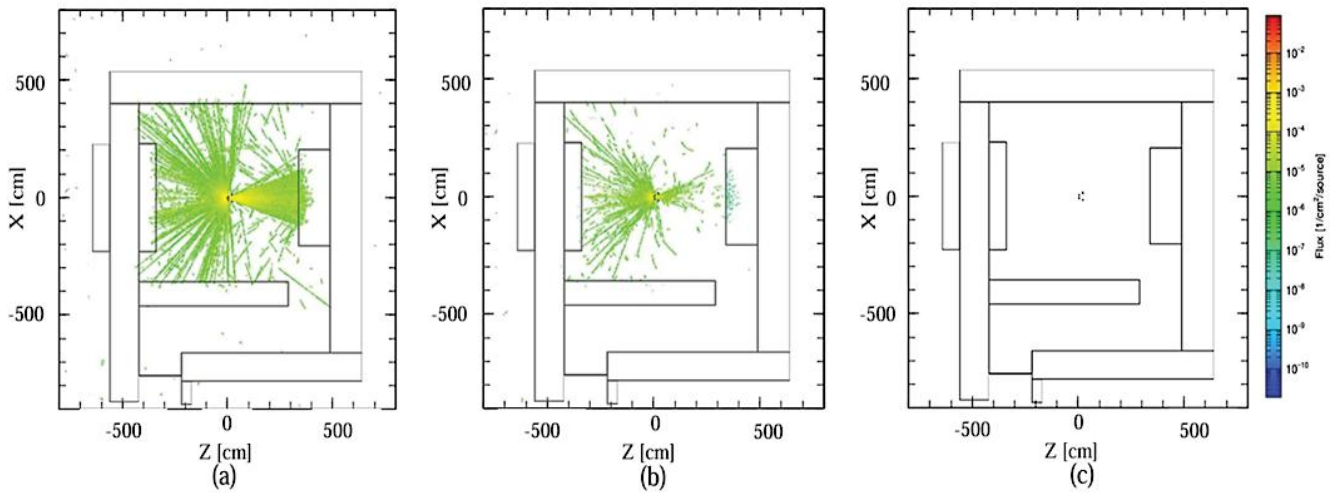

Fig. 6: 2D visualization of (a) photon tracking, (b) electron tracking and (c) neutron tracking within the bunker (XZ plane). The color scale represents flux intensity.

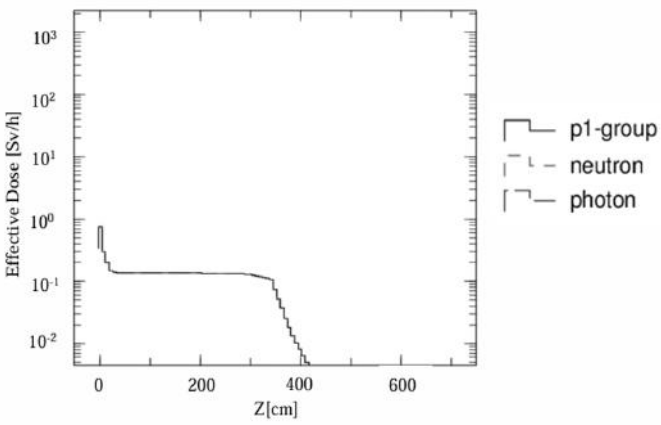

Fig.7: Dose mapping across the shielding bunker, showing effective dose attenuation.

Along with, **Fig. 7** presents the effective dose distribution along the z-axis inside the shielding structure. Photon dose, illustrated by the blue curve, starts with a rapid decrease, maintains stability until ~350 cm, and then experiences a quick drop beyond 400 cm. Neutron contribution (red dashed) is negligible, confirming no significant photo-neutron production at 6 MV. The p1-group curve is similar to the photon curve, confirming photons are the main contributor. The flat part shows scattered photons, and the rapid decrease beyond 400 cm proves the shielding is effective. Overall, photon transport shapes the dose, and the shielding provides adequate protection.

4. Conclusions

This study successfully proved the application of the PHITS Monte Carlo code in medical physics for LINAC modeling and bunker shielding design. A detailed and validated model of the Varian CLINAC (iX) 6 MV head accurately simulated photon and electron production and transport, with simulated PDD and beam profile data. The simulations further confirmed the absence of neutron production at 6 MV, in line with theoretical expectations. Finally, the designed bunker shielding featuring concrete and lead proved highly effective, as Monte Carlo results confirmed that the primary and secondary barriers together with the maze attenuate radiation to levels well below regulatory safety limits.

This work demonstrates how Monte Carlo (MC) simulations can be used for practical applications beyond traditional research and education, such as verifying new radiotherapy equipment, analyzing complex scenarios, and optimizing radiation shielding. Future studies will focus on extending the model to include multi-leaf collimators (MLCs), modeling higher energies (15 MV) where neutron production is significant, simulating electron beam modes, and integrating the model into more complex treatment planning scenarios.

References

1. Zeman EM, Schreiber EC and Tepper JE; Basics of radiation therapy. In Abeloff's clinical oncology: 431-460 (2020).
2. Chargari C, Deutsch E, Blanchard P, Gouy S, Martelli H, Guérin F, Dumas I, Bossi A, Morice P, Viswanathan AN and Haie-Meder C; Brachytherapy: An overview for clinicians. CA: a cancer journal for clinicians, 69(5): 386-401(2019).
3. Khan, FM and Gibbons JP; Khan's the physics of radiation therapy. Lippincott Williams & Wilkins (2014).
4. Seco J and Verhaegen F; eds. Monte Carlo techniques in radiation therapy. Boca Raton: CRC press 334, (2013).
5. Fix MK, Keall PJ, Dawson K and Siebers JV; Monte Carlo source model for photon beam radiotherapy: photon source characteristics: Monte Carlo source model, Med. Phys., 31(11): 3106-3121 (2004).
6. Hedin E, Bäck A, Swanpalmer J and Chakarova R; Monte Carlo simulation of linear accelerator Varian Clinac iX. Report MFT-Radfys 1(1), (2010).

7. National Committee on Radiation Protection (US). Structural shielding design for medical x-ray imaging facilities. National Council on Radiation Protection and Measurements (2004).
8. Linton OW and Mettler Jr FA; National council on radiation protection and measurements. In National conference on dose reduction in CT, with an emphasis on pediatric patients, AJR Am J. Roentgenol, 181(2): 321-329 (2003).
9. Ródenas J, Martinavarro A, León A and Verdú G; Application of the Monte Carlo method to shielding analysis in medical linear accelerators, J. Nucl. Sci. Tech., 37(1): 441-445 (2000).
10. Furuta T and Sato T; Medical application of particle and heavy ion transport code system PHITS. Radio. Phys. Tech., 14(3): 215-225 (2021).
11. Sato T, Niita K, Matsuda N, Hashimoto S, Iwamoto Y, Noda S, Ogawa T, Iwase H, Nakashima H, Fukahori T and Okumura K; Particle and heavy ion transport code system, PHITS, version 2.52. J. Nucl. Sci. Techn., 50(9): 913-923 (2013).
12. Abou-Taleb WM, Hassan MH, El_Mallah EA and Kotb SM; MCNP5 evaluation of photoneutron production from the Alexandria University 15 MV Elekta Precise medical LINAC, App. Rad. and Isot., 135:184-191 (2018).
13. Kumer T, Das PK, Khatun R, Rahman MA, Akter S and Roy SK; Comparative studies of absolute dose in water phantom, solid water phantom and MatriXX with MULTICube phantom. Int. J. Med. Phys., Clinical Engineering and Radiation Oncology, 10(4): 169-177 (2021).
14. Martin-Martin G, Walter S and Guibelalde E; Dosimetric impact of failing to apply correction factors to ion recombination in percentage depth dose measurements and the volume-averaging effect in flattening filter-free beams, Physica Medica, 77: 176-180 (2021).
15. Hossain M and Rhoades J; On beam quality and flatness of radiotherapy megavoltage photon beams, Aust. Physi. & Eng. Sci. Medi., 39(1):135-145 (2016).
16. Bieda MR, Antolak JA and Hogstrom KR; The effect of scattering foil parameters on electron-beam Monte Carlo calculations, Med. Phys., 28(12): 2527-2534 (2001).
17. Bilalodin B and Abdullatif F; Modeling and analysis of percentage depth dose (PDD) and dose profile of x-ray beam produced by linac device with voltage variation, Jurnal Ilmiah Teknik Elektro Komputer dan Informatika (JITEKI), 8(2): 206-214 (2022).
18. Jabbari I and Monadi S; Development and validation of MCNPX-based Monte Carlo treatment plan verification system, J. of Med. Phys., 40(2): 80-89 (2015).
19. Yani S, Dirgayussa IGE, Rhani MF, Soh RC, Haryanto F and Arif I; Monte Carlo study on electron contamination and output factors of small field dosimetry in 6 MV photon beam, Smart Science, 4(2): 87-94 (2016).
20. Anam C, Soejoko DS, Haryanto F, Yani S and Dougherty G; Electron contamination for 6 MV photon beams from an Elekta linac: Monte Carlo simulation, J. Phys. Appli., 2(2): 97-101 (2020).
21. Patil BJ, Chavan ST, Pethe SN, Krishnan R, Bhoraskar VN and Dhole SD; Simulation of e–γ–n targets by FLUKA and measurement of neutron flux at various angles for accelerator-based neutron source, Ann. Nucl. Ener., 37(10): 1369-1377 (2010).